SSRG International Journal of Electronics and Communication Engineering
ISSN: 2348-8549/ https://doi.org/10.14445/23488549/IJECE-V10I5P104

Volume 10 Issue 5, 38-48, May 2023
© 2023 Seventh Sense Research Group®

Original Article

Study and Analysis of Thermal Imaging Sensors for Object Detection

B. Shubha[1], V. Veena Devi Shastrimath[2]

[1, 2]*Department of Electronics and Communication Engineering, NITTE (Deemed to be University), NMAM Institute of Technology, Nitte, Karnataka, India.*

[1]*Corresponding Author : shubhab@nitte.edu.in*

Received: 05 March 2023 Revised: 10 April 2023 Accepted: 05 May 2023 Published: 31 May 2023

Abstract *- Low-resolution thermal imaging sensors are extensively used for applications where human privacy needs to be protected, and continuous monitoring is essential. Thermal sensors are increasingly used in indoor environmental applications like health monitoring, security, and innovative housing. Such sensors provide low-resolution images. However, these low-resolution images are sufficient to detect the objects. This paper studies and analyses two thermal imaging sensors by considering their characteristics, detection capability, and performance. It recommends the type of sensor to be used in specific applications. The received data from the sensor is processed, and image enhancement is carried out using the interpolation technique. Human detection is achieved by removing the background noise and converting the Image to binary. The experiments were conducted in the laboratory using Grid-EYE and MLX90640 thermopile sensors to detect the human in real-time. The processing of the sensor data is implemented using Raspberry Pi.*

Keywords *- Filtering, Interpolation, Raspberry Pi, Thermopile image sensor, Thermal image.*

1. Introduction

Object detection and estimation are widely used in intelligent control scenarios. Sensors are typically used to detect the positions and movements of people. Optical imaging techniques are widely used to observe the movement and tracking of people [1]. However, with optical imaging, it is not possible to hide the identity of people in such situations; privacy will not be guaranteed. This paper uses a thermal sensor-based technique to detect a human's presence, which helps maintain privacy. Commonly used thermal sensors are Passive Infrared (PIR) sensors and Thermopile sensors. The ability of the PIR sensors to detect the target depends on measuring the change in temperature of the moving object and has the limitation of detecting the stationary object. The other widely used thermal sensor is the thermopile sensor, which detects moving and stationary objects [2]. As the detection is carried out with the help of a temperature gradient, thermal imaging sensors protect privacy. Since this technique is very cost-effective, it is used for indoor applications like health monitoring, security, and detection [3].

The two commonly available thermal imaging sensors with different prices, resolutions, and characteristics are the Grid-EYE sensor [4] and the MLX90640 sensor [5]. This manuscript performs a comparative study of these two low-resolution thermal sensors. The experimental study is carried out to check the different characteristics like resolution, detection area, and distance. The detection algorithm is implemented using both sensors, and its performance is checked. An algorithm is designed only for indoor applications like meeting rooms, offices, and health monitoring. Based on the results, one can select the best suitable sensors for their application. The multiple objects are detected using MLX90640 more accurately than the Grid-EYE sensor.

Very few studies are being carried out to compare the performance of thermal imaging sensors. In the recent past, many systems have emerged out of Grid-EYE sensors. Another thermal sensor, MLX90640, has better resolution than the Grid-Eye sensor and is slowly gaining popularity. So far, a few implementations using Grid-EYE sensors like – the detection of finger movement by keeping a small distance between the finger and sensor [6], and the detection and tracking of the human by keeping the sensor on the ceiling and the door [7, 8]. However, in all the developments, the analysis is done on the offline data. The MLX90640 sensor detects and monitors workers' activity in an office and predicts the range between humans and the sensor [9-13]. Machine learning algorithms were used to analyze the activity of workers. The complexity of detection algorithms is more significant than this article's proposed algorithm. In the paper [14], three sensors (Grid-EYE, MLX90640, and Lepton) are compared by considering the sensor characteristics like resolution, warm-up time, noise figures, and detection range. Many of the existing methods are done with sensors kept on the ceiling. The significant modifications done in this study are keeping the sensors on the side wall of the room, which covers more detection area, and all the experiments are carried out in real-time using Raspberry Pi to detect the object. To study the performance in detail, extensive experiments are conducted. Various experiments include single and multiple object detection and contour size variation for near and far objects. The article is ordered as follows: The detection algorithm of the object is presented in the next section. The section results and discussion give different plots of the algorithm for single and multiple objects. Also, compare the results of both sensors. Finally, the summary of the result and future scope is included in the conclusion section.

2. Thermal Imaging Sensor

Thermal sensors provide temperature variations in the sensor's Field of View (FOV). This paper tries to study the properties of two sensors (Grid-EYE and MLX90460) and arrive at a conclusion to suggest a suitable sensor for a given application.

2.1. Grid-EYE Sensor

Grid-EYE sensor (AMG8833) is an infrared thermopile sensor with 8x8 resolution with a FOV of 60°. It detects the temperature range of $-20^{\circ}C$ to $100^{\circ}C$ at a low gain [4]. The sensor kept on a $3m$ height ceiling will have a detection area of approximately $9m^2$ on the floor. The maximum detection range claimed by the manufacturer is $7m$. The chip receives radiation from the heated objects and is amplified and converted to a digital signal. The converted data is stored in the sensor's memory and can be read from the sensor using the I2C protocol. The frame rate of the sensor could be configured as 10 FPS (Frame Per Second) or 1 FPS. The sensor takes 15 seconds to warm up and has a temperature accuracy of $\pm 3^{\circ}C$.

2.2. MLX90460 Sensor

The MLX90640 infrared thermopile sensor has a resolution of 32x24 with a FOV of 55° x 35° and measuring the temperature range of $-40^{\circ}C$ to $300^{\circ}C$. The radiated heat signals of the object are amplified and converted to digital signals. It consists of an I2C interface with different programmable refresh rates from $0.5\,Hz$ to $64\,Hz$. The warm-up time required for the sensor to stabilize 4 minutes [5], with a temperature accuracy of $\pm 3^{\circ}C$.

3. Methodology

Object detection is a process of identifying the presence of an object in the FOV of a sensor. The steps involved in detecting an object in an indoor environment are as in Figure 1. The serial data from the sensor is received and converted into the temperature. Received data from the sensor is in 8x8 (for Grid -EYE) and 32x24 (for MLX90640) grid form. In the beginning, the background frame of an empty room is captured, and then the current frame with the object is captured. In the presence of a human, the Image will contain pixels with higher values at the target position surrounded by pixels with lower values. Then it is processed by applying the interpolation methods to resize the thermal Image. Different interpolation methods like Nearest Neighbor, Bilinear and Bicubic Interpolation are available. The literature shows that bicubic interpolation is the best algorithm for detection [13] applications. Further, the background noise in the Image is removed by performing background subtraction and filtering. The background subtraction process minimizes the multiple peaks present in the Image, and filtering is performed to smoothen the Image. Then at every 10 seconds again, the updated background temperature is calculated. Finally, the Image is converted into a binary to detect the active pixels. Active pixels represent the human objects present in the data frame of the sensor's thermal Image.

3.1. Bicubic Interpolation

The Grid-EYE thermal image sensor output data frame resolution is 8x8, and MLX90640 thermal image sensor output data frame is 32x24. Since the resolution of the data frame of both sensors is low, it is increased to 100x100 by using Bicubic Interpolation. The pixel value is determined by taking a weighted average of the 16 neighboring pixels [15,16]. The bicubic interpolation is implemented using the Kernel [17],

$$K(i) = \begin{cases} \frac{3}{2}|i|^3 - \frac{5}{2}|i|^2 + 10 \leq |i| < 1 \\ \frac{-1}{2}|i|^3 + \frac{5}{2}|i|^2 - 4|i| + 21 \leq |i| < 2 \\ 02 < |i| \end{cases} \tag{1}$$

Where i is the distance between the current pixel and interpolated pixel value. The Bicubic interpolation, $B_i(i,j)$ is defined by [18,19]:

$$B_i(i,\mathrm{j}) = \sum_{m=0}^{3}\sum_{n=0}^{3} a_{mn} i^m j^n \tag{2}$$

The new interpolated value is calculated from 16 coefficients. a_{mn} , of its neighboring four-pixel location derivatives. The i and j are the locations of the new interpolated pixel.

3.2. Active Pixel Detection and Noise Removal

The active frame is subtracted from the interpolated background frame to calculate the active pixels in the frame. This process will help to remove the information pertaining to the ambient temperature from the image frame.

The subtracted Image $B_s(i,\text{j})$ could be calculated as:

$$B_s(i,\text{j}) = T(i,\text{j}) - \frac{1}{N}\sum_{g=1}^{N} B^g(i,\text{j}) \quad (3)$$

Where, $T(i,\text{j})$ is the input thermal image of the sensor with a target. The mean of the background image $B^g(i,j)$ of N data frames are subtracted from the current data frame. Upon removing the static noise, the target is properly visible in the extracted foreground image [14]. Further, the data frames are smoothened by applying a Gaussian filter $g(i,j)$ is [20- 22]:

$$g(i,j) = \frac{1}{2\pi\sigma^2} e^{-\left(\frac{i^2+j^2}{2\sigma^2}\right)} \quad (4)$$

σ is the standard deviation with a mean equal to 0. The filter mask of Gaussian distribution, g is given by:

$$g = \frac{1}{16}\begin{bmatrix} 1 & 2 & 1 \\ 2 & 4 & 2 \\ 1 & 2 & 1 \end{bmatrix} \quad (5)$$

In this study, the standard deviation of the filter is kept at 3. Gaussian filtering of an input image T with size MxN is given by:

$$G(i,j) = \sum_{s=-\text{p}}^{q} \sum_{t=-\text{p}}^{q} g(s,t) T(i+s, j+t) \quad (6)$$

Where g is the filter mask of size pxq, the i and j are the indices of the input thermal image. Each pixel (s,t) in g overlaps with each pixel (i,j) in T.

3.3. Binary Thermal Image

The filtered Image is changed to the binary thermal Image by calculating the appropriate threshold value. T_h. The adaptive threshold value is dynamically computed as

$$T_h = PeakValue \quad (7)$$

The $PeakValue$ is the maximum value in each of the frames. If the target exists in the detection area, its temperature values will be higher than the background. If the pixel value in the foreground image is higher than the threshold value, it is considered as '1'; else '0'. This conversion provides the object's location in the binary Image [23-24]. In the binary thermal Image, only the large area of '1' represents the object.

4. Results and Discussion

4.1. Experimental Setup

The research was conducted in a laboratory environment where both the sensors are mounted on the side wall of a room, as in Figure 2. Each sensor covers a different detection area due to the different FOV. First, the research considers a single person to check the sensor characteristics like resolution, detection area, temperature values, and target size. The area covered by the Grid-EYE and MLX90460 sensors is as in Figure 3. Since the FOV of both sensors differs, they are mounted at different heights on the wall to cover the maximum detection area. The sensor is strategically placed in a suitable position. This article uses the Raspberry Pi 4 (RPI) development module for interfacing the sensor. RPI is a low-cost single-board computer with high processing, computational power and could be used in control applications. It gives easy access to a 40-pin GPIO extension header, making it appropriate to connect several sensors to the system. RPI also supports Wi-Fi and Bluetooth interfaces [25-27].

4.2. Object Detection Algorithm Performance

In the beginning, the algorithm is tested using a single object in the FOV of a sensor, as in Figure 4. The outcomes of different stages of the algorithm to detect a single person using a Grid-EYE sensor and MLX90640 sensor at a distance of 1m from the sensor are shown in Figure 5 and Figure 6. The experiment is extended to three and five objects; the results are shown in Figure 7 to Figure 12. It can be observed that the MLX90460 sensor has a better resolution. In the binary thermal Image, active pixels indicate the target's location.

From the result, it is noticed that using the Grid-EYE sensor makes it difficult to differentiate the number of objects in the detection area where the MLX90640 sensor gives better. In the MLX90640 thermal Image, the number of objects is properly visible in the thermal Image and is easy to detect compared to the Grid-Eye sensor. If the distance between the human targets is small, then the Grid-EYE sensor will recognize them as a single object, whereas the MLX90640 sensor will recognize them as separate as long as the targets do not overlap.

4.3. Distance Versus Object Size

As the object moves away from the sensor, the size of the object decreases. Results of the Grid- EYE sensor at different distances of $1m$, $2m$, and $2.5m$ are shown in Figure 13. Also, the results using the MLX90460 sensor at different distances of $1m$, $2.5m$, and $4m$ are shown in Figure 14. From the results, it is observed that using the Grid-EYE sensor, it is difficult to sense an object beyond $3m$ whereas the MLX90640 can detect adequately up to a distance of $4m$ between the sensor and the object. The object's size is reduced as the range between the object and the sensor increases. The reduction of the active pixel contour area as the object moves far from the sensor is shown in Figure 15. These results calculate the maximum and minimum range and size of the object for detection.

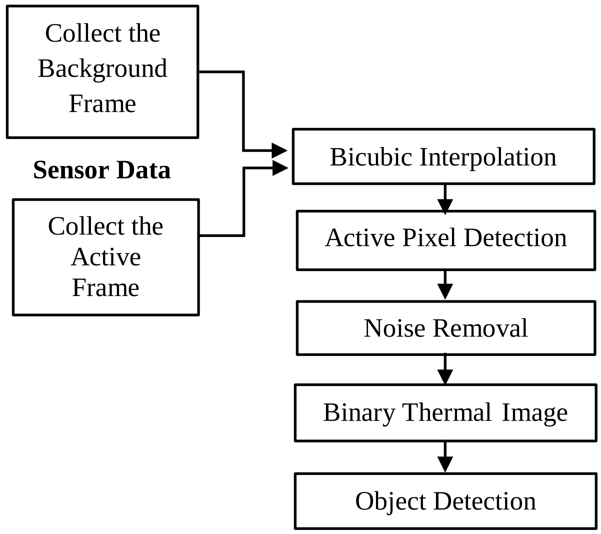

Fig. 1 Object detection steps

Fig. 2 Experimental setup

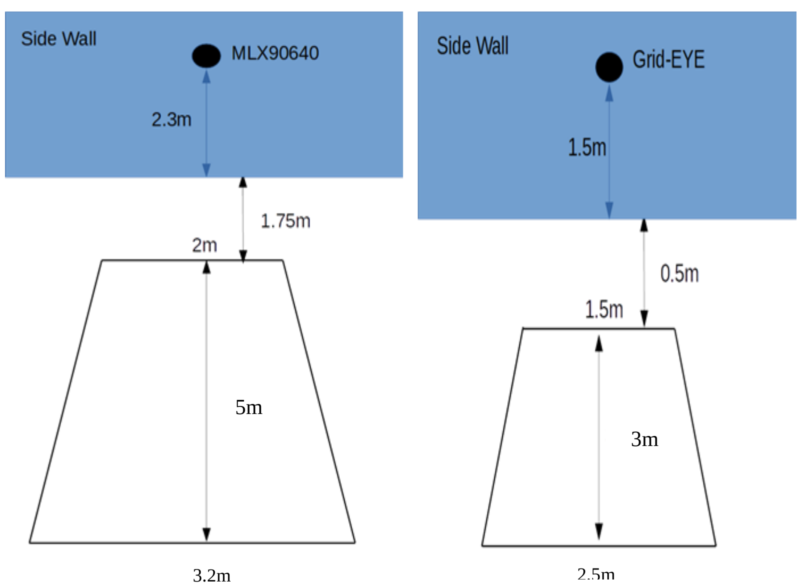

Fig. 3 Detection area of the sensors (a) MLX90640 sensor (b) Grid-EYE sensor

Fig. 4 Optical age of single object

Grid-EYE Sensor

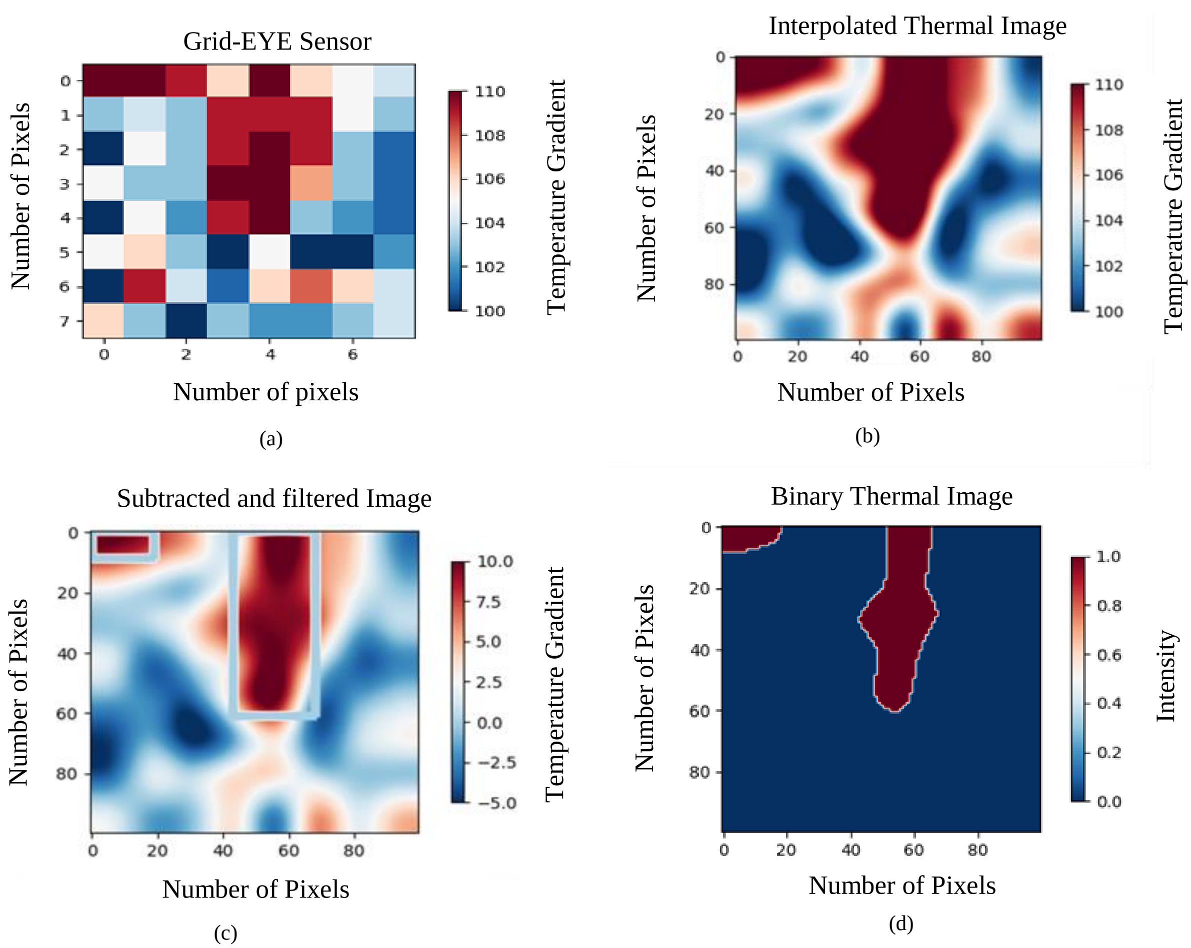

Fig. 5 Single object detection using Grid-EYE sensor (a) Unprocessed image, (b) Interpolated image, (c) Subtracted and filtered image, (d) Binary image

MLX90640

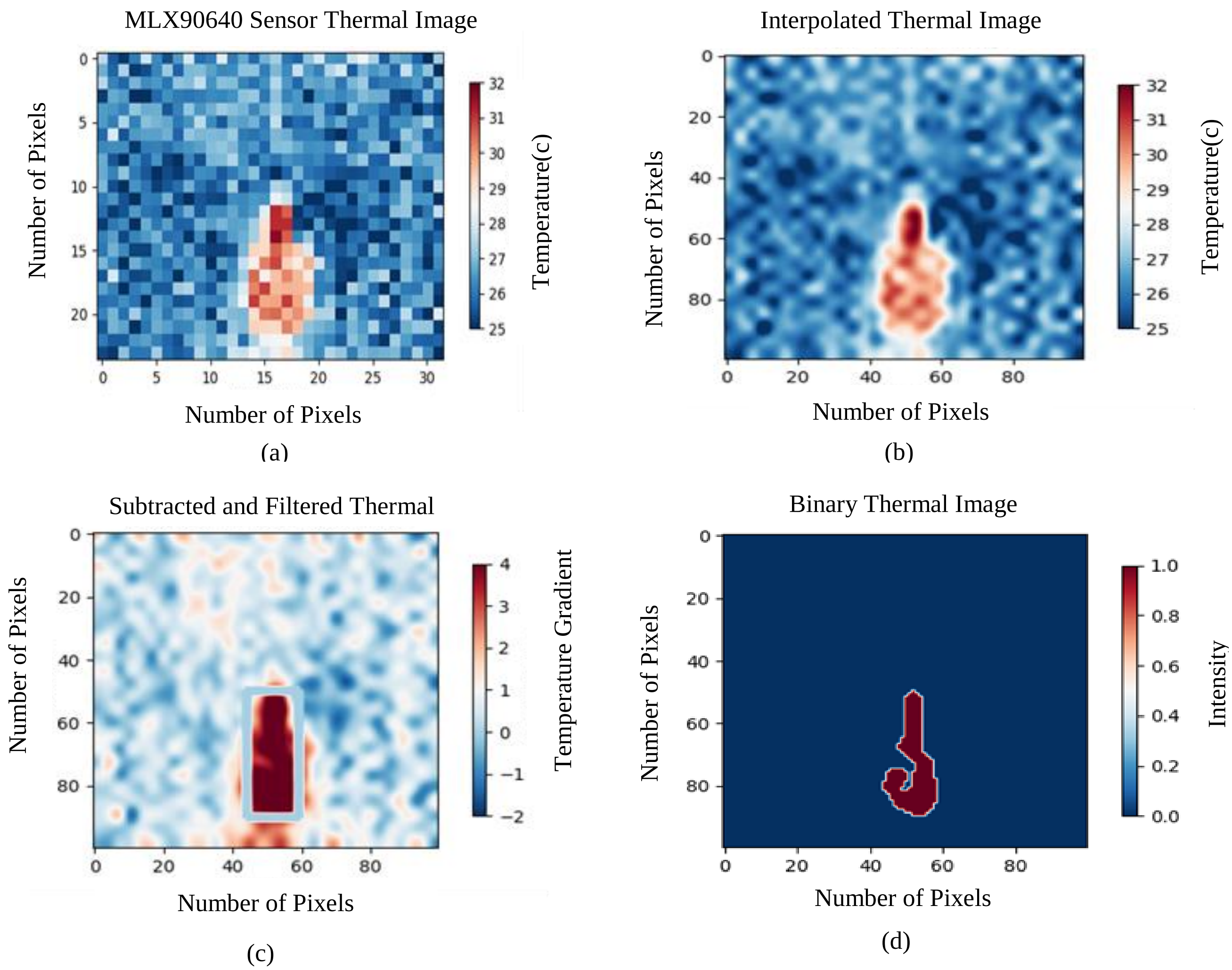

Fig. 6 Single object detection using MLX90640 sensor (a) Unprocessed Image, (b) Interpolated image, (c) Subtracted and filtered image, (d) Binary image

Fig. 7 Optical image of three objects

Grid-EYE

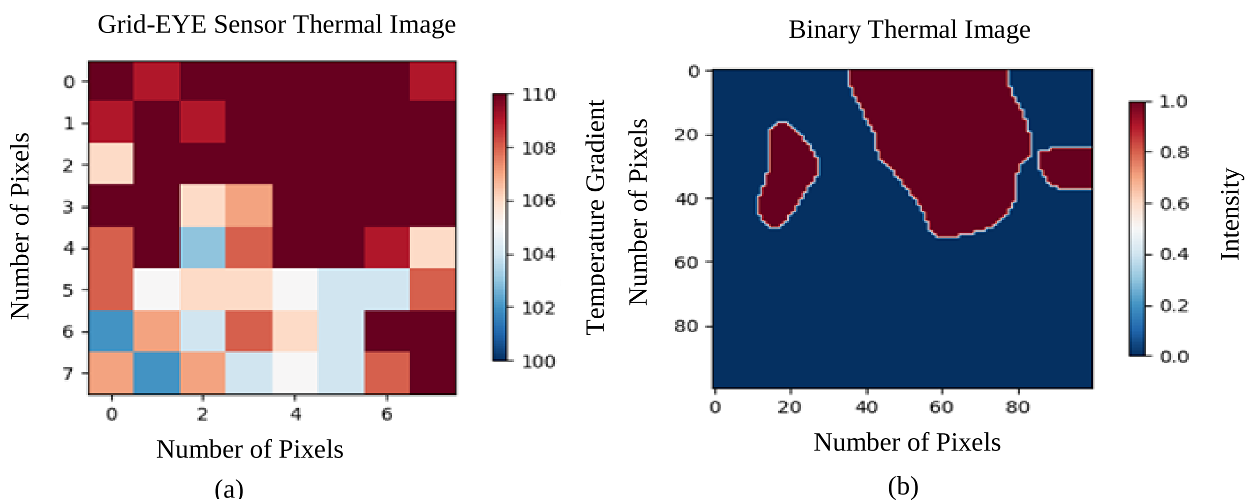

Fig. 8 Three objects detection using the Grid-EYE sensor (a) Unprocessed image, (b) Binary image MLX90640

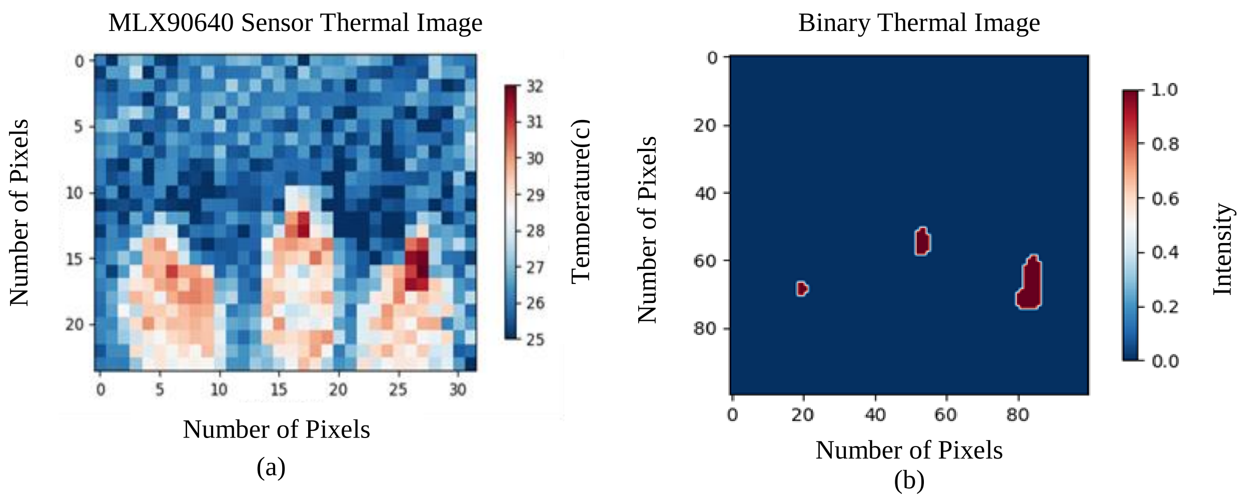

Fig. 9 Three objects detection using the MLX90640 sensor (a) Unprocessed image, (b) Binary image

Fig. 10 Optical image of five objects

Grid-EYE Sensor

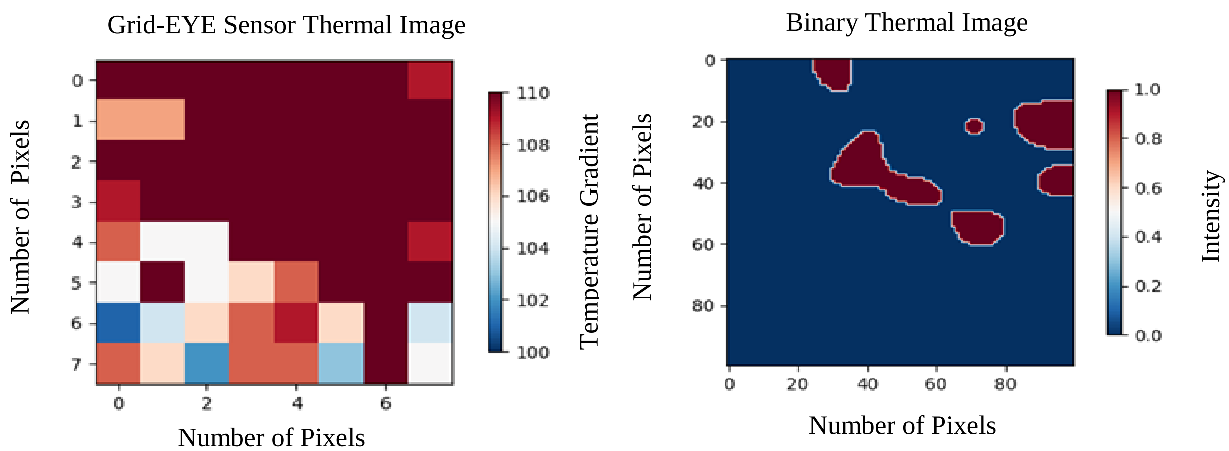

(a) (b)

Fig. 11 Five objects detection using the Grid-EYE sensor (a) Unprocessed image, (b) Binary image MLX90640 Sensor

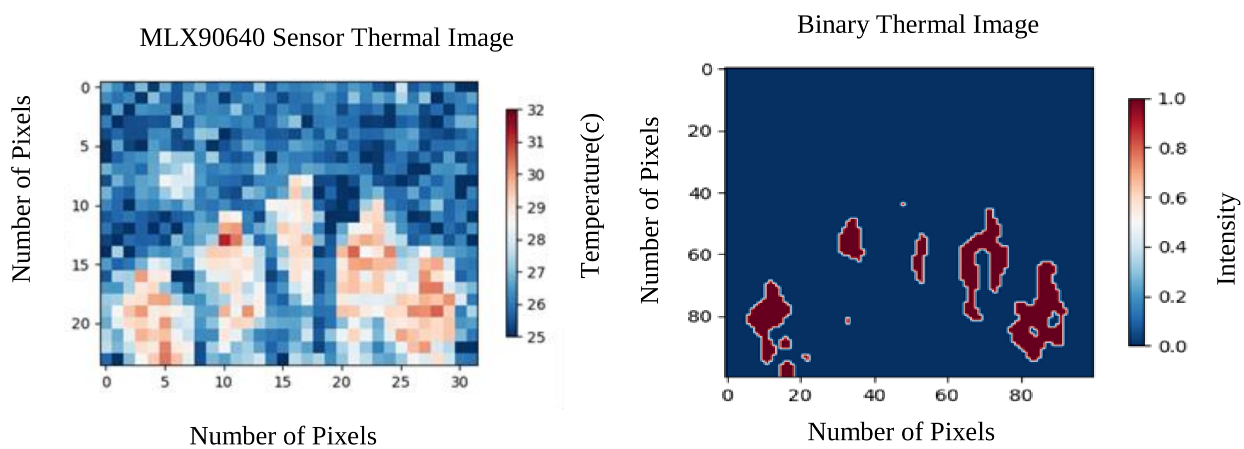

(a) (b)

Fig. 12 Five objects detection using MLX90640 sensor (a) Unprocessed image, (b) Binary image Grid-EYE Sensor

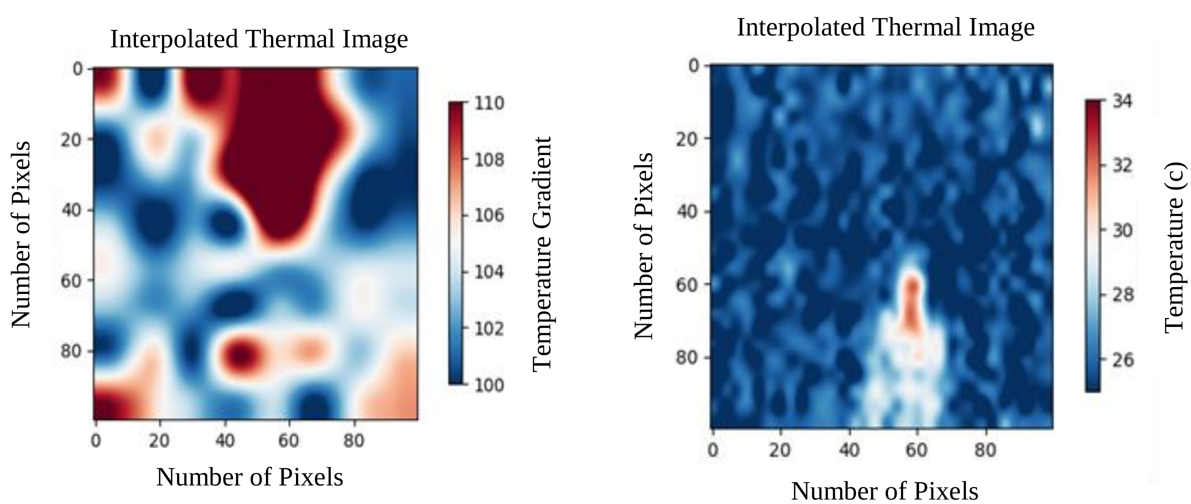

(a) (a)

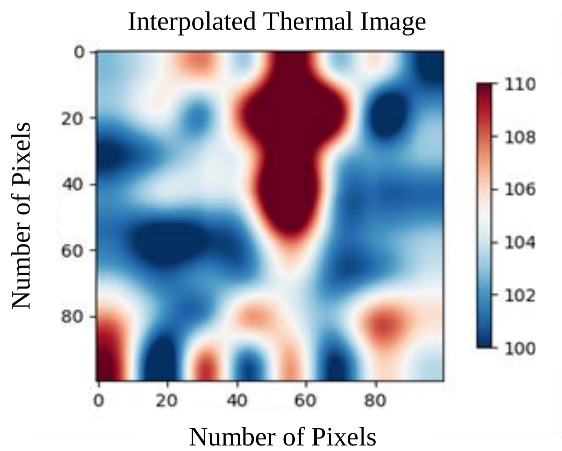

(b)

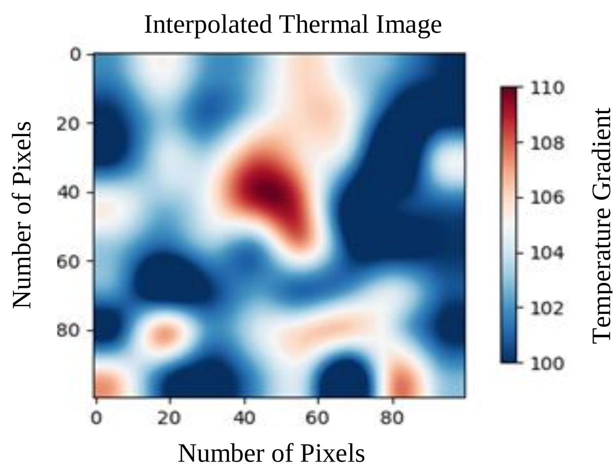

(c)

Fig. 13 Distance versus object size using Grid-EYE (a) Distance = $1m$, (b) Distance = $2m$, (c) Distance = $2.5m$ MLX90640 Sensor

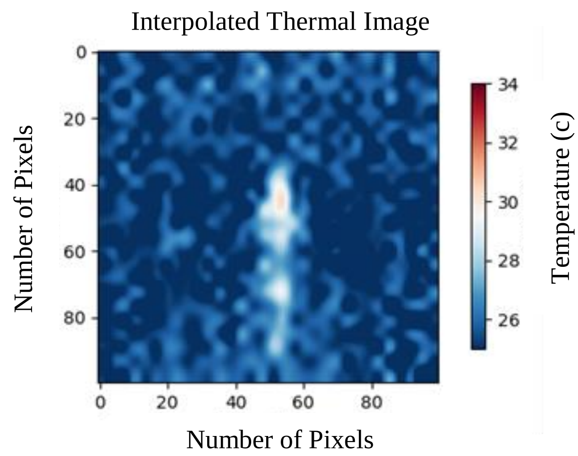

(b)

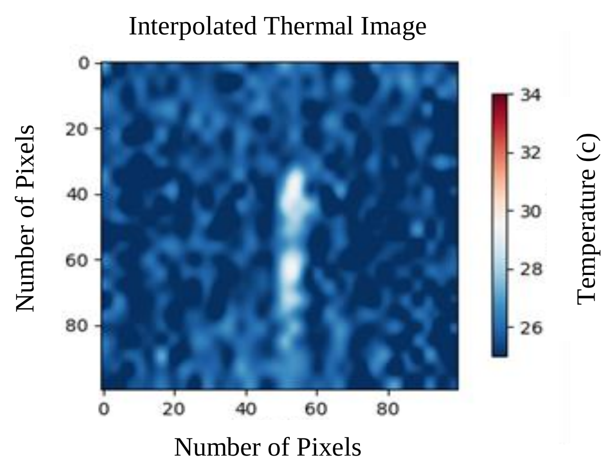

(c)

Fig. 14 Distance versus object size using MLX90640 (a) Distance = $1m$, (b) Distance = $2.5m$, (c) Distance = $4m$

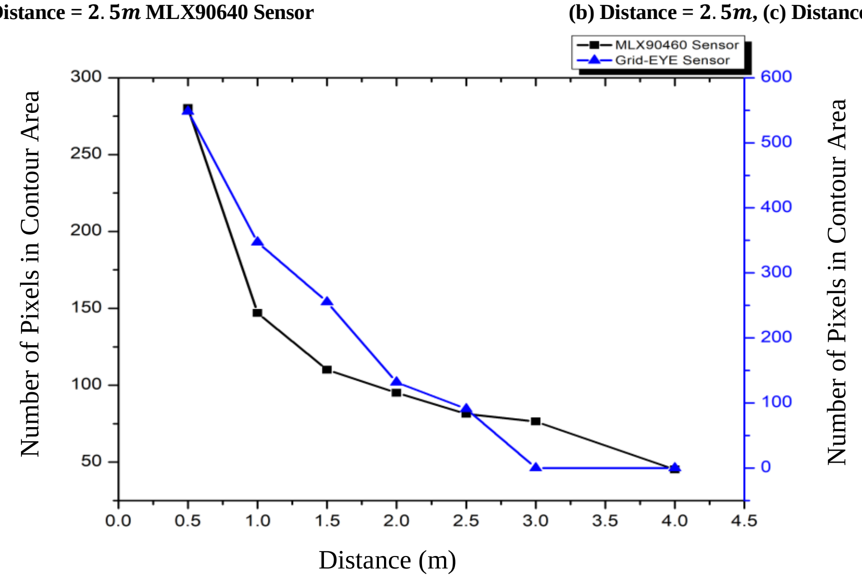

Fig. 15 Distance versus contour area size

5. Conclusion

This paper focuses on comparing the two low-resolution thermal imaging sensors. Some sensor characteristics like resolution, FOV, and detection range were initially tested and compared. Then the performance of the algorithm to detect the object is compared.

From the detection algorithm, it is concluded that, as the number of people in the detection area increased, the Grid-EYE sensor failed to detect the same as there was an overlap in the thermal Image. In contrast, in MLX90640 thermal image, the object could be differentiated easily. The size of the detected area reduces as the distance between the sensor and the human increases.

Among the two thermal sensors, it is concluded that the MLX90640 sensor performance is better compared to the Grid-EYE sensor. From these performance results, one can select a Grid-EYE sensor for applications involving only one or two object detection, whereas MLX90640 could be chosen for applications involving the detection of many objects with better resolution. The study could be extended to possibly employ more sensors to span the larger area with inter-sensor communication.

Acknowledgments

The authors acknowledge the Research Innovation Center of NMAM Institute of Technology for providing the space to collect thermal sensor data.

References

[1] Seigo Kanazawa et al., "A Fuzzy Automated Object Classification by Infrared Laser Camera," *Proceedings of SPIE - The International Society for Optical Engineering, Security and Sensing*, vol. 8058, 2011. [CrossRef] [Google Scholar] [Publisher Link]

[2] B. Shubha, V. Veena Devi Shastrimath, and L. V. Prabhu, "Parameter Analysis of Pyroelectric and Thermopile Detectors," *International Conference for Emerging Technology (INCET)*, pp. 1-7, 2020. [CrossRef] [Google Scholar] [Publisher Link]

[3] Claudia Chiţu et al., "Wireless System for Occupancy Modeling and Prediction in Smart Buildings," *25th Mediterranean Conference on Control and Automation (MED)*, pp. 1094-1099, 2017. [CrossRef] [Google Scholar] [Publisher Link]

[4] Panasonic Industry, Infrared Array Sensor Grid-EYE. [Online]. Available: https://industrial.panasonic.com

[5] Melexis, MLX90640 32x24 IR Array *Datasheet*, 2018. [Online]. Available:https://www.melexis.com

[6] Akshaya D. Shetty et al., "Detection and Tracking of a Human Using the Infrared Thermopile Array Sensor - "Grid-EYE"," *International Conference on Intelligent Computing, Instrumentation and Control Technologies (ICICICT)*, pp. 1490-1495, 2017. [CrossRef] [Google Scholar] [Publisher Link]

[7] Dongning Qu, Bo Yang, and Nanhao Gu, "Indoor Multiple Human Targets Localization and Tracking Using Thermopile Sensor," *Infrared Physics & Technology*, vol. 97, pp. 349–359, 2019. [CrossRef] [Google Scholar] [Publisher Link]

[8] Abdallah Naser, Ahmad Lotfi, and Joni Zhong, "Towards Human Distance Estimation Using a Thermal Sensor Array," *Neural Computing and Applications*, 2021. [CrossRef] [Google Scholar] [Publisher Link]

[9] Hessam Mohammadmoradi et al., "Measuring People-Flow Through Doorways Using Easy-to-Install IR Array Sensors," *13th International Conference on Distributed Computing in Sensor Systems (DCOSS)*, pp. 35-43, 2017. [CrossRef] [Google Scholar] [Publisher Link]

[10] Congcong Ma et al., "Work Engagement Recognition in Smart Office," *Procedia Computer Science*, vol. 200, pp. 451-460, 2022. [CrossRef] [Google Scholar] [Publisher Link]

[11] Cristian Perra et al., "Monitoring Indoor People Presence in Buildings using Low-Cost Infrared Sensor Array in Doorways," *Sensors*, vol. 21, no. 12, pp. 4062, 2021. [CrossRef] [Google Scholar] [Publisher Link]

[12] Mika Maaspuro, "Infrared Occupancy Detection Technologies in Building Automation-A Review," *ARPN Journal of Engineering and Applied Sciences*, vol. 13, no. 19, pp. 8055–8068, 2018. [Google Scholar] [Publisher Link]

[13] Veena Chidurala, and Xinrong Li, "Detection of Moving Objects using Thermal Imaging Sensors for Occupancy Estimation," *Internet of Things*, vol. 17, p. 100487, 2022. [CrossRef] [Google Scholar] [Publisher Link]

[14] Veena Chidurala, and Xinrong Li, "Occupancy Estimation Using Thermal Imaging Sensors and Machine Learning Algorithms," *In IEEE Sensors Journal*, vol. 21, no. 6, pp. 8627-8638, 2021. [CrossRef] [Google Scholar] [Publisher Link]

[15] V. Diana Earshia, and M. Sumathi, "A Comprehensive Study of 1D and 2D Image Interpolation Techniques," *International Conference on Communications and Cyber Physical Engineering (ICCCE)*, pp. 383-391, 2018. [CrossRef] [Google Scholar] [Publisher Link]

[16] Richard Alan Peters II, *Image Processing* Lecture Notes: Resizing Images, 2015. [Online]. Available: https://ia902707.us.archive.org/23/items/Lectures_on_Image_Processing/EECE_4353_15_Resampling.pdf

[17] B. Shubha, and V. Veena Devi Shastrimath, "Real-Time Occupancy Detection System using Low-Resolution Thermopile Array Sensor for Indoor Environment," *IEEE Access*, vol. 10, pp. 130981-130995, 2022. [CrossRef] [Google Scholar] [Publisher Link]

[18] Liu Liu, Yue Chen, and Bo Yan, "An Efficient Classification-Based Image Interpolation Algorithm," *4th International Congress on Image and Signal Processing*, pp. 1063-1066, 2011. [CrossRef] [Google Scholar] [Publisher Link]

[19] Rafael C. Gonzalez, and Richard E. Woods, *Digital Image Processing*, 3rd edition, Prentice Hall, 2008. [Online]. Available: https://www.academia.edu/67778643/Digital_Image_Processing_Third_Edition
[20] Gaussian Filtering. [Online]. Available: https://homepages.inf.ed.ac.uk/rbf/HIPR2/gsmooth.htm
[21] Gaussian Filter. [Online]. Available: https://link.springer.com/content/pdf/10.1007/978-1-84800-297-5_5.pdf
[22] Anna A. Trofimova et al., "Indoor Human Detection Based on Thermal Array Sensor Data and Adaptive Background Estimation," *Journal of Computer and Communications*, vol. 5, no. 4, pp.16-28, 2017. [CrossRef] [Google Scholar] [Publisher Link]
[23] Payel Roy et al., "Adaptive Thresholding: A Comparative Study," *2014 International Conference on Control, Instrumentation, Communication and Computational Technologies (ICCICCT)*, pp. 1182-1186, 2014. [CrossRef] [Google Scholar] [Publisher Link]
[24] Sheikh Ferdoush, and Xinrong Li, "Wireless Sensor Network System Design using Raspberry Pi and Arduino for Environmental Monitoring Applications," *Procedia Computer Science*, vol. 34, pp. 103-110, 2014. [CrossRef] [Google Scholar] [Publisher Link]
[25] Raspberry Pi 4 Tech Specs. [Online]. Available: https://www.raspberrypi.com/products/raspberry-pi-4-model-/specifications
[26] Priyadharshini S., S.Natarajan, and S.Kavitha, "USB Device Driver Development of Image Processing Using Raspberry Pi 4 via Thingspeak," *SSRG International Journal of Electronics and Communication Engineering*, vol. 8, no. 6, pp. 1-3, 2021. [CrossRef] [Publisher Link]
[27] Chandan A D et al., "Survey Paper on Vehicle Security using Facial Recognition & Password," *SSRG International Journal of Electronics and Communication Engineering*, vol. 9, no. 6, pp. 5-9, 2022. [CrossRef] [Publisher Link]
[28] V. Teju, and D. Bhavana, "An Efficient Object Tracking in Thermal Imaging Using Optimal Kalman Filter," *International Journal of Engineering Trends and Technology*, vol. 69, no. 12, pp. 197-202, 2021. [CrossRef] [Publisher Link]
[29] Sudhir Dagar, and Geeta Nijhawan, "Area Efficient Moving Object Detection using Spatial and Temporal Method in FPGA," *International Journal of Engineering Trends and Technology*, vol. 70, no. 9, pp. 138-147, 2022. [CrossRef] [Publisher Link]
[30] V.Vivek et al., "Development of Abandoned Object Detection Based on Region of Interest Method," *International Journal of Computer and Organization Trends*, vol. 8, no. 6, pp. 1-6, 2018. [Publisher Link]
[31] D. J. Samatha Naidu, and B. Lakshmi Devi, "Vehicle Speed Tracking Detection using Gaussian Mixture Models," *SSRG International Journal of Mobile Computing and Application*, vol. 9, no. 3, pp. 1-4, 2022. [CrossRef] [Publisher Link]
[32] Esmaeil Mirmahdi, and Omid Ghorbani Shirazi, "Installation of Suitable Sensors for Object Detection and Height Control on Combine Harvester," *SSRG International Journal of Mechanical Engineering*, vol. 8, no. 5, pp. 12-19, 2021. [CrossRef] [Google Scholar] [Publisher Link]